

Article

A 2D Membrane MEMS Device Model with Fringing Field: Curvature-Dependent Electrostatic Field and Optimal Control

Paolo Di Barba ¹, Luisa Fattorusso ² and Mario Versaci ^{3,*}

¹ Dipartimento di Ingegneria Industriale e dell'Informazione, University of Pavia, Via A. Ferrata 5, 27100 Pavia, Italy; paolo.dibarba@unipv.it

² Dipartimento di Ingegneria dell'Informazione Infrastrutture Energia Sostenibile, "Mediterranea" University, Via Graziella Feo di Vito, 89124 Reggio Calabria, Italy; luisa.fattorusso@unirc.it

³ Dipartimento di Ingegneria Civile Energia Ambiente e Materiali, "Mediterranea" University, Via Graziella Feo di Vito, 89124 Reggio Calabria, Italy

* Correspondence: mario.versaci@unirc.it; Tel.: +39-096-5169-2273

Abstract: An important problem in membrane micro-electric-mechanical-system (MEMS) modeling is the fringing-field phenomenon, of which the main effect consists of force-line deformation of electrostatic field E near the edges of the plates, producing the anomalous deformation of the membrane when external voltage V is applied. In the framework of a 2D circular membrane MEMS, representing the fringing-field effect depending on $|\nabla u|^2$ with the u profile of the membrane, and since strong E produces strong deformation of the membrane, we consider $|E|$ proportional to the mean curvature of the membrane, obtaining a new nonlinear second-order differential model without explicit singularities. In this paper, the main purpose was the analytical study of this model, obtaining an algebraic condition ensuring the existence of at least one solution for it that depends on both the electromechanical properties of the material constituting the membrane and the positive parameter δ that weighs the terms $|\nabla u|^2$. However, even if the the study of the model did not ensure the uniqueness of the solution, it made it possible to achieve the goal of finding a stable equilibrium position. Moreover, a range of admissible values of V were obtained in order, on the one hand, to win the mechanical inertia of the membrane and, on the other hand, to ensure that the membrane did not touch the upper disk of the device. Lastly, some optimal control conditions based on the variation of potential energy are presented and discussed.

Keywords: membrane MEMS; semilinear elliptic 2D boundary value problems; mean curvature; Bessel equations; stability; optimal control



Citation: Di Barba, P.; Fattorusso, L.; Versaci, M. A 2D Membrane MEMS Device Model with Fringing Field: Curvature-Dependent Electrostatic Field and Optimal Control. *Mathematics* **2021**, *9*, 465. <https://doi.org/10.3390/math9050465>

Academic Editor: Carlos Llopis-Albert

Received: 10 February 2021

Accepted: 22 February 2021

Published: 25 February 2021

Publisher's Note: MDPI stays neutral with regard to jurisdictional claims in published maps and institutional affiliations.



Copyright: © 2021 by the authors. Licensee MDPI, Basel, Switzerland. This article is an open access article distributed under the terms and conditions of the Creative Commons Attribution (CC BY) license (<https://creativecommons.org/licenses/by/4.0/>).

1. Introduction

The remarkable development of embedded technologies in recent years is, in large part, due to the small size of the devices used that manage the link between the physical nature of the problem and the logic of the machine language [1,2]. In this context, interest in micro-electro-mechanical system (MEMS) devices has been very high since they represent a good approximation of the human-machine interface [3]. MEMS are devices that have been recognized as one of the most promising of the 21st century, capable of revolutionizing both the industrial and the consumer-product worlds. MEMS are devices integrated in miniaturized form on the same substrate as that of semiconductor material (silicon), combining the electrical properties of the integrated semiconductor with optomechanical properties [1]. These are "intelligent" systems that combine electronic, optical, biological, chemical, and mechanical fluid management functions in a very small space, integrating sensor and actuator technology, and the most diverse process-management functions [1,3]. MEMS technologies are adopted in the most varied application fields, many of which are based on microscopic mirrors [1,2] or oscillating lenses in a single or array version that are used to create complex optoelectronic devices [2]. In microwave electronics,

MEMS devices are often used as single switches for complex applications such as matching networks, resonant filters, power-supply networks for array antennas, and generally reconfigurable systems [2]. MEMS are also used for new solutions in chemistry and bio-engineering [2]. Since the first batch device was produced [4], technological development has strongly influenced the production of physicomathematical models, describing increasingly complex multiphysics [5–7]. However, such models, although theoretically valid, rarely provide explicit solutions, so that the conditions of existence and uniqueness of the solution need to be obtained with reasonable computational costs [8–10]. Furthermore, if the solution is not analytically obtainable, one can rely on numerical techniques that provide approximate solutions that, if they satisfy the aforementioned conditions of existence and uniqueness [11–13], do not represent ghost solutions [14–18]. The scientific community is currently working hard both on the analysis and synthesis of multiphysical models, and on technology transfer [19–24]. In such contexts, it is preferred to study MEMS devices equipped with symmetries in order to obtain models that can be studied more easily, both mathematically and physically [12]. Thus, for application reasons, the authors focus their attention on a 2D circular membrane MEMS device used in many industrial and biomedical applications [1,12,25–28]. Particularly, the authors consider a bounded circular smooth domain Ω , where a 2D circular membrane MEMS device is represented by two parallel disks placed d apart [12]. Furthermore, an electrically conductive elastic membrane (which has the same size as the disks at rest) was clumped on the edge of the lower disk (which acted as a support to the membrane) deforming toward the upper disk when an external electric voltage V is applied between the disks. This deformation, in this work, is described by the profile of the membrane, $u(r)$, $r \in [0, R]$, with r being the radial coordinate [1,5,6,11]. The model took the following well-known form [1,5,6,11]:

$$\begin{cases} \Delta u(r) = -\frac{\lambda^2}{(1-u(r))^2} \\ u(R) = 0, \quad u'(0) = 0, \\ 0 < u(r) < d \end{cases} \quad (1)$$

in which λ^2 is a parameter depending on V . However, electrostatically, if $d \not\ll R$, the fringing-field phenomenon occurs [29–31]. In other words, the lines of force of electric field \mathbf{E} away from the edges of the device appear parallel and uniform, while as one approaches the edges of the disks, they become a curve [29–31]. Thus, with these premises, in Model (1), λ^2 becomes $\lambda^2(1 + \delta|\nabla u(r)|^2)$ where term $\delta|\nabla u(r)|^2$, with $\delta \in \mathbb{R}^+$, considers the fringing-field effects (when $\delta = 0$, no fringing field phenomenon is observed). Since the device presents radial symmetry with respect to vertical axes $r = 0$, in $\Delta u(r)$, only the radial component is taken into account, and $\nabla u(r) = u'(r)$. Upon deformation of the membrane, the electrostatic capacitance of the device varies, as the distance between the membrane and upper disk is variable. Furthermore, $\frac{\lambda^2}{(1-u(r))^2} \propto |\mathbf{E}|^2$, so that $\frac{\lambda^2}{(1-u(r))^2} = \theta|\mathbf{E}|^2$, $\theta \in \mathbb{R}^+$ [11]. Moreover, physically, \mathbf{E} on the membrane is locally orthogonal to the straight-line tangent to the profile of the membrane. Thus, it makes sense to consider $|\mathbf{E}|$ proportional to mean curvature $K(r, u(r))$ of the membrane [12]. So, as detailed in Section 3, the model becomes the following 2D second-order semilinear elliptic model:

$$\begin{cases} u''(r) = -\frac{1}{r}u'(r) - \frac{4(1-u(r)-d^*)^2}{\theta\lambda^2(1+\delta|u'(r)|^2)} \\ u(R) = 0, \quad u'(0) = 0, \\ 0 < u(r) < d, \end{cases} \quad (2)$$

in which d^* is the critical security distance ensuring that the membrane does not touch the upper disk. In recent years, there has been an interesting surge in the application of machine learning and statistical frameworks to solve similar problems as those in this paper, as highlighted in the studies shown in [32–34]. Model (2) is very difficult to solve and, in any cases, does not give explicit solutions, so that we focus on if any conditions ensuring

both the existence and uniqueness of the solution are obtainable. In particular, considering Model (2) in a more general formulation, an interesting result of the existence of at least one solution is obtained if an algebraic condition, depending on the electromechanical properties of the material constituting the membrane and fringing-field parameter δ , is satisfied. However, although the uniqueness of the solution is not ensured, the unique admitted equilibrium position results in being stable. Moreover, the range of admissible values of V , to both win the mechanical inertia of the membrane $(V_{min})_{inertia}$ and to avoid the membrane touching the upper disk $(V_{max})_{permissible}$, is achieved and discussed. Lastly, some optimal control conditions, formulated in terms of variation of potential energy, are discussed. In order to improve the readability of the paper, Figure 1 shows a schematic flowchart of the entire work.

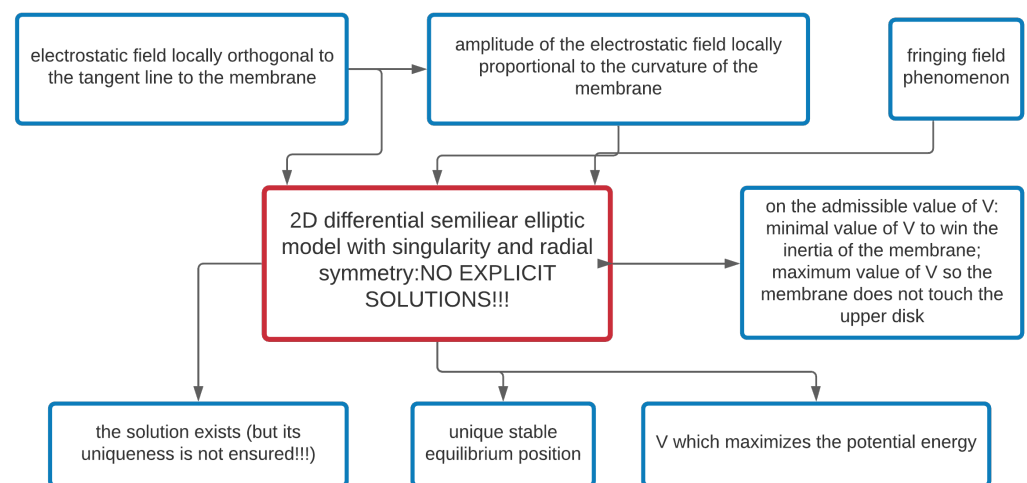


Figure 1. Work flowchart.

2. Circular-Membrane MEMS Devices: Overview

The MEMS device studied in this paper consisted of two parallel metal disks of which the radius is R , placed at a distance d between them [12]. A circular membrane of radius R in its rest condition was anchored to the edges of the lower disk (which acted as a support). The membrane, under the effect of an external V , deformed towards the upper plate without touching it. Then, \mathbf{E} in the device generated electrostatic pressure $p_{el} = 0.5\epsilon_0|\mathbf{E}|^2$ (ϵ_0 , permittivity of free space) that deflected the membrane. Electrostatically, when the membrane deformed, \mathbf{E} , which depended on the distance between membrane and upper disk, was locally orthogonal to the line tangent to the membrane at the point. Furthermore, the electrostatic capacitance of the device, C_{el} , was also variable, as the distance between membrane and upper disk locally varied. The higher $|\mathbf{E}|$ was, the greater the curvature of the membrane, so that $|\mathbf{E}|$ was proportional to curvature K of the membrane.

2.1. Circular-Membrane MEMS as Transducer

For our purposes, we exploited some similarities with the model of a MEMS circular plate transducer subjected to mechanical pressure p .

Remark 1. Usually, the terms “sensor” and “transducer” are used interchangeably. However, a distinction must be made, as a sensor is a sensitive element that converts an input into a physical output, which is acquired into an electrical signal. On the other hand, a transducer consists of an input interface, a sensor, and an output interface. In this paper, we refer to a MEMS transducer in order to consider both interfaces.

In this section, we report some important results concerning the mechanics, as already discussed in [12], of when a metal plate is subjected to mechanical pressure p , deforms, and its deflection u satisfies the known equation [1,35]

$$\rho hu_{tt} - T\Delta u + D\Delta^2 u = 0 \tag{3}$$

with ρ being the density of the material constituting the plate, with thickness h , T , and [35]

$$D = \frac{Yh^3}{12(1 - \nu^2)}, \tag{4}$$

with Y (Young’s modulus) and ν (Poisson ratio) being the mechanical tension and flexural stiffness of the plate, respectively. Moreover, if the plate is circular, u only depends on radial coordinate r (assuming radial symmetry). With these premises, and in steady-state conditions, u is valuable as [1,35]

$$u(r) = \frac{R^4}{64D} \left(1 - \left(\frac{r}{R}\right)^2\right)^2 p \tag{5}$$

with $0 \leq r \leq R$, for z -directed u [35]. Of course, if $r = 0$, displacement at the center of the plate u_0 becomes [1,35]

$$u_0 = \frac{R^4}{64D} p \tag{6}$$

so that (5) becomes [1]

$$u(r) = u_0 \left(1 - \left(\frac{r}{R}\right)^2\right)^2 p. \tag{7}$$

Then, unlike the actuator, the device works like a transducer. In fact, as verified in [12], p generates $u(r)$, so that C_{el} becomes [1,35]

$$C_{el}(u_0) = \int_0^R \frac{2\epsilon_0\pi r}{d\left(1 - \frac{u(r)}{d}\right)} dr, \quad \text{if } |u_0| \ll d. \tag{8}$$

Both h and D are limited values. Then, $u(r)$ becomes inconspicuous, so that the distance between the two plates remains d . Using the Taylor series (up to the third term) and considering the electrostatic capacitance at equilibrium, $C_0 = \epsilon_0 \frac{\pi R^2}{d}$ for $p = 0$, Equation (8) becomes [35]

$$C_{el}(u_0) \approx C_0 \left(1 + \frac{u_0}{3d} + \frac{u_0^2}{5d^2}\right), \tag{9}$$

which can be exploited to achieve the coenergy of the system, the charge in the membrane, and the electrical force [11]. Furthermore, in [12], $C_{el}(u_0)$, as computed in (9), is a nonlinear function of u_0 . Moreover, $\frac{dC_{el}(u_0)}{du_0} \propto p$ by electrostatic force f_{el} . In other words, $\frac{dC_{el}(u_0)}{du_0} \approx \frac{2f_{el}}{V^2}$, and, if $|u_0| \ll d$

$$|\mathbf{E}(r)| \approx \frac{V}{d - u_0 \left(1 - \left(\frac{r}{R}\right)^2\right)^2}. \tag{10}$$

All involved physical quantities depend on d because the circular plate had a significant value of D ; then, $u(r)$ was extremely limited, so that any dependencies on $d - u(r)$ could be replaced by the simpler dependence on d . If, instead of the deformable plate, a membrane was considered (see [12]), h is negligible, so that D , as formulated in (4) significantly decreases compared to the case in which a deformable plate is present. Considering that the lower the D value, the more flexible the membrane, u_0 became higher with the risk

that the membrane touched the upper plate. In this, it is imperative to consider $d - u(r)$ in the denominator of (9). By subjecting the membrane to p , $u(r)$ becomes [1]

$$u(r) = u_0 \left(1 - \left(\frac{r}{R} \right)^2 \right) \tag{11}$$

with

$$u_0 = \frac{pR^2}{4T}. \tag{12}$$

In this case, f_{el} became [1,35]

$$f_{el} = \frac{0.5\epsilon_0\pi R^2 V^2}{(d - u(r))^2} \tag{13}$$

from which

$$p_{el} \cong \frac{f_{el}}{\pi R^2} = \frac{0.5\epsilon_0 V^2}{(d - u(r))^2}. \tag{14}$$

Remark 2. In the calculation of f_{el} and p_{el} , the surface of the membrane was approximated as πR^2 , even in the presence of membrane deformation. This approximation is justifiable because $d \ll R$, and the surface of the deformed membrane could then be approximated to the surface of the membrane in the rest position.

2.2. p and p_{el} : An Interesting Relationship

The relationship between p and p_{el} arises from, when V is applied, \mathbf{E} is generated inside the device, also generating p_{el} , which deforms the membrane, obtaining $u(r)$ and making it clear that there is a link between p and p_{el} . Let us first observe that, from (12), u_0 depends on p and, setting

$$k_1 = \frac{R^2}{4T}, \tag{15}$$

we can write:

$$u_0 = \frac{pR^2}{4T} = k_1 p. \tag{16}$$

If there are no further stresses, p originates exclusively from p_{el} , which, in turn, is generated by $|\mathbf{E}|$. Then, the following chain of equalities makes sense:

$$u_0 = k_1 p = k_1 k_2 p_{el} = k p_{el}, \tag{17}$$

with both k_2 and k being constant.

Remark 3. Considering (14), u_0 becomes

$$u_0 = k p_{el} = \frac{k\epsilon_0 V^2}{2(d - u(r))^2} \tag{18}$$

where $d - u(r)$ is locally the distance between membrane and upper disk. The profile of the membrane must also absolutely not touch the upper disk. Then, once the membrane is deformed,

$$u(r) \leq d - d^*, \tag{19}$$

must occur, so that

$$\frac{1}{(d - u(r))^2} \leq \frac{1}{d^{*2}}. \tag{20}$$

Graphical details are shown in Figure 2. Thus, Equation (11), considering Equation (18) and Remark 3, can be written as

$$u(r) \leq \bar{u}(r) = \frac{k\epsilon_0 V^2}{2d^{*2}} \left(1 - \left(\frac{r}{R}\right)^2\right). \tag{21}$$

The relationship between p and p_{el} constitutes a dual transducer–actuator model. So, the behavior of the transducer helps us to understand the function of an actuator and vice versa.

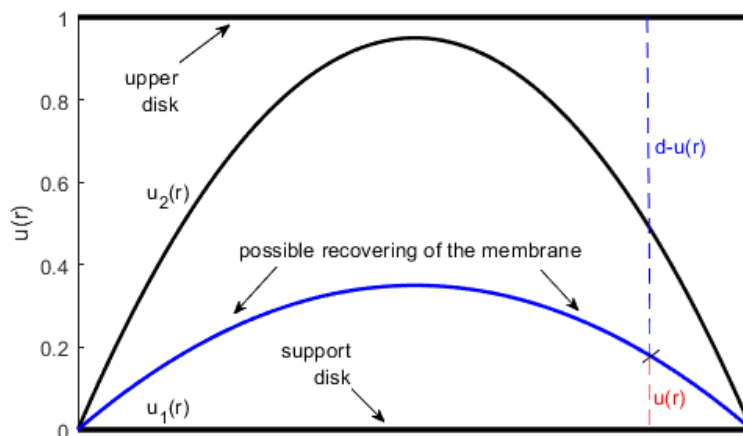


Figure 2. $u_1(r)$ and $u_2(r)$ for model (2).

Remark 4. Equation (21) is a very important relationship because it represents an upper solution that is useful to exploit a lemma known in the literature to obtain an algebraic condition governing the existence of the solution for (2).

3. Problem Formulation

As introduced above, Model (1), in the presence of a fringing field, becomes

$$\begin{cases} \Delta u(r) = -\frac{\lambda^2(1+\delta|\nabla u(r)|^2)}{(1-u(r))^2} \\ u(R) = 0, \quad u'(0) = 0, \\ 0 < u(r) < d, \end{cases} \tag{22}$$

highlighting a radial symmetry with respect to vertical axes $r = 0$, $\Delta u(r) = \frac{1}{r}u'(r) + u''(r)$. Moreover, with $\nabla u(r) = u'(r)$, Equation (22) can be written as

$$\begin{cases} \frac{1}{r}u'(r) + u''(r) = -\frac{\lambda^2(1+\delta|u'(r)|^2)}{(1-u(r))^2} \\ u(R) = 0, \quad u'(0) = 0, \\ 0 < u(r) < d. \end{cases} \tag{23}$$

Furthermore, when the membrane deformed, the electrostatic capacitance of the device varied, as the distance between membrane and upper disk was variable. Moreover, in (23), $\frac{\lambda^2}{(1-u(r))^2} \propto |\mathbf{E}|^2$, so that it makes sense to write $\frac{\lambda^2}{(1-u(r))^2} = \theta|\mathbf{E}|^2$, $\theta \in \mathbb{R}^+$ [11]. Thus, Equation (23) becomes

$$\begin{cases} u''(r) + \frac{1}{r}u'(r) = -\theta|\mathbf{E}|^2(1 + \delta|u'(r)|^2) \\ u(R) = 0, \quad u'(0) = 0 \\ \theta \in \mathbb{R}^+, \quad 0 < u(r) < d. \end{cases} \tag{24}$$

In addition, \mathbf{E} on the membrane was physically locally orthogonal to the straight-line tangent to the profile of the membrane, so that $|\mathbf{E}|$ could be considered proportional to mean curvature $K(r, u(r))$ of the membrane [12]

$$K(r, u(r)) = \frac{1}{2} \left(u''(r) + \frac{1}{r} u'(r) \right) \tag{25}$$

The larger $|\mathbf{E}|$ is, the more the membrane deforms. Then, it makes sense to assume that $|\mathbf{E}| \propto K(r, u(r))$ (as detailed in (25)). Thus,

$$|\mathbf{E}| = \mu(r, u(r), \lambda) K(r, u(r)) \tag{26}$$

where $\mu(r, u(r), \lambda)$, the function of proportionality, can be written as [11,12]

$$\mu(r, u(r), \lambda) = \frac{\lambda}{(1 - u(r) - d^*)} \tag{27}$$

with $\mu(r, u(r)) \in C^0(A)$ and $A = [-\mathbb{R}, \mathbb{R}] \times [0, 1)$, and, in the radial symmetry framework, $K(r, u(r))$ represents the mean curvature, so that (26), considering both (27) and (25), can be written as

$$|\mathbf{E}|^2 = \frac{1}{4} \frac{\lambda^2}{(1 - u(r) - d^*)^2} \left(u''(r) + \frac{1}{r} u'(r) \right)^2 \tag{28}$$

and Model (24) becomes

$$\begin{cases} u''(r) + \frac{1}{r} u'(r) = -\frac{\theta \lambda^2}{4(1 - u(r) - d^*)^2} \left(u''(r) + \frac{1}{r} u'(r) \right)^2 (1 + \delta |u'(r)|^2) \\ u(R) = 0, \quad u'(0) = 0 \\ \theta \in \mathbb{R}^+, \quad 0 < u(r) < d. \end{cases} \tag{29}$$

Therefore, from (29), Equation (2) follows.

Remark 5. Equation (2) was achieved from (29) because it was easy to prove that $u''(r) + \frac{1}{r} u'(r) \neq 0$. For details, see [12].

4. General Problem Formulation

Model (2) is a special case of the following general problem:

$$\begin{cases} u''(r) + F(r, u(r), u'(r)) = 0 \\ u(b) = B, \quad u'(a) = m, \end{cases} \tag{30}$$

in which $F \in C^0((a, b] \times \mathbb{R} \times \mathbb{R})$ and $B, m \in \mathbb{R}$. In fact, setting

$$F(r, u(r), u'(r)) = \frac{1}{r} u'(r) + \frac{4(1 - u(r) - d^*)^2}{\theta \lambda^2 (1 + \delta |u'(r)|^2)}, \tag{31}$$

$$B = m = 0 \tag{32}$$

and

$$b = R, \quad a = 0 \tag{33}$$

we obtain (2). Now, we obtain conditions ensuring both the existence and uniqueness of the solution for (2). We introduce two preliminary lemmas.

5. Preliminary Lemmas

For further details, see [36]). Particularly, we exploited Lemma 1 to prove that (2) admits at least one solution. On the other hand, Lemma 2 was used to prove that the solution for (2) is not unique.

Lemma 1. Let us consider Model (30) and two twice continuously differentiable functions $u_1(r)$ and $u_2(r)$, such that

$$u_1(r) < u_2(r), \quad r \in (a, b). \tag{34}$$

Let us also consider

$$u_1''(r) + F(r, u_1(r), u_1'(r)) > 0 \tag{35}$$

and

$$u_2''(r) + F(r, u_2(r), u_2'(r)) < 0 \tag{36}$$

for $r \in (a, b)$. Furthermore, let $F(r, y(r), y'(r))$ be a continuous function satisfying the following Lipschitz condition:

$$\begin{aligned} &K_1(r)(u(r) - v(r)) + L_2(r)(u'(r) - v'(r)) \\ &\leq F(r, u(r), u'(r)) - F(r, v(r), v'(r)) \\ &\leq K_2(r)(u(r) - v(r)) + L_1(r)(u'(r) - v'(r)) \end{aligned} \tag{37}$$

in $\mathcal{U} \times (-\infty, +\infty)$ in which

$$\mathcal{U} = \{(r, u) : a < r < b \text{ and } u_1(r) \leq u(r) \leq u_2(r)\} \tag{38}$$

and $K_1(r), K_2(r), L_1(r)$ and $L_2(r)$ are continuous functions in $(a, b]$. If $u_1'(a) \geq u_2'(a)$, with $u_1(b) = u_2(b) = B$, Equation (30) has at least one solution, $u(r)$, such that $u_1(r) \leq u(r) \leq u_2(r)$ in $[a, b]$.

Lemma 2. Let us suppose that the conditions of Lemma 1 are satisfied, and $u_1(r)$ and $u_2(r)$ satisfy the boundary conditions. Let us also suppose that

$$u''(r) + K_2(r)u(r) + L_1(r)u'(r) = 0 \tag{39}$$

has no nontrivial solution that satisfies zero-boundary conditions on any subinterval of $[a, b]$; then, Equation (30) has only one solution, $u(r)$, such that $u_1(r) \leq u(r) \leq u_2(r)$.

6. An Interesting Result of the Existence of at Least One Solution

In this section, we prove the existence of at least one solution for (2), referring to Section 7, the discussion on uniqueness.

Theorem 1. Let us consider Problem (2). Let us also consider $u_1(r)$ and $u_2(r)$ as two functions twice continuously differentiable and both defined on $[0, R]$, such that $u_1(r) < u_2(r)$. Moreover, let us suppose that

$$u_1''(r) + \frac{1}{r}u_1'(r) + \frac{4(1 - u_1(r) - d^*)^2}{\theta\lambda^2(1 + \delta|u_1'(r)|^2)} > 0 \tag{40}$$

and

$$u_2''(r) + \frac{1}{r}u_2'(r) + \frac{4(1 - u_2(r) - d^*)^2}{\theta\lambda^2(1 + \delta|u_2'(r)|^2)} < 0 \tag{41}$$

for $r \in (0, R)$. Furthermore, if $\frac{1}{r}u'(r) + \frac{4(1-u(r)-d^*)^2}{\theta\lambda^2(1+\delta|u'(r)|^2)}$ is a continuous function (obviously, except for $r = 0$), which satisfies the Lipschitz condition in $\mathcal{U} \times (-\infty, +\infty)$, with $\mathcal{U} = \{(r, u) : 0 < r < R \text{ and } u_1(r) \leq u(r) \leq u_2(r)\}$, and if $u_1'(0) \geq u_2'(0)$, with $u_1(R) = u_2(R) = 0$ with

$$\theta\lambda^2 > \frac{2d^{*2}R^2}{k\epsilon_0V^2\left(1 + \delta\left(\frac{k\epsilon_0V^2r}{d^{*2}R^2}\right)^2\right)}; \tag{42}$$

thus, Problem (2) admits at least one solution.

Proof of Theorem 1. To prove this theorem, we need to exploit Lemma 1. Particularly, we assume that

$$u_1(r) = 0, \quad \forall r \in [0, R] \tag{43}$$

and

$$u_2(r) = \bar{u}(r) = \frac{k\epsilon_0 V^2}{2d^{*2}} \left(1 - \left(\frac{r}{R}\right)^2\right). \tag{44}$$

as derived from (21). Figure 2 displays both $u_1(r)$ and $u_2(r)$, a possible recovery of the membrane. By construction, it is clear that $u_1(r) < u_2(r)$; moreover, they are twice continuously differentiable functions. We easily observe that $u_1'(r) = u_1''(r) = 0$, so that

$$u_1''(r) + \frac{1}{r}u_1'(r) + \frac{4(1 - u_1(r) - d^*)^2}{\theta\lambda^2(1 + \delta|u_1'(r)|^2)} = \frac{(1 - d^*)^2}{\theta\lambda^2} > 0. \tag{45}$$

Thus, (40) is verified. Moreover,

$$u_2'(r) = -\frac{k\epsilon_0 V^2 r}{d^{*2} R^2} \tag{46}$$

and

$$u_2''(r) = -\frac{k\epsilon_0 V^2}{d^{*2} R^2} \tag{47}$$

so that we need to verify (41), which becomes

$$\begin{aligned} & u_2''(r) + \frac{1}{r}u_2'(r) + \frac{4(1 - u_2(r) - d^*)^2}{\theta\lambda^2(1 + \delta|u_2'(r)|^2)} \\ &= -2\frac{k\epsilon_0 V^2}{d^{*2} R^2} + \frac{4\left(1 - \frac{k\epsilon_0 V^2}{2d^{*2}}\left(1 - \left(\frac{r}{R}\right)^2\right) - d^*\right)^2}{\theta\lambda^2\left(1 + \delta\left(\frac{k\epsilon_0 V^2 r}{d^{*2} R^2}\right)^2\right)} < 0 \end{aligned} \tag{48}$$

that is

$$\frac{4\left(1 - \frac{k\epsilon_0 V^2}{2d^{*2}}\left(1 - \left(\frac{r}{R}\right)^2\right) - d^*\right)^2}{\theta\lambda^2\left(1 + \delta\left(\frac{k\epsilon_0 V^2 r}{d^{*2} R^2}\right)^2\right)} < 2\frac{k\epsilon_0 V^2}{d^{*2} R^2}. \tag{49}$$

For this purpose, since (49) $0 \leq \left(1 - \frac{k\epsilon_0 V^2}{2d^{*2}}\left(1 - \left(\frac{r}{R}\right)^2\right) - d^*\right)^2 < 1$, to verify (41) and then (48), it is sufficient to impose

$$\frac{1}{\theta\lambda^2\left(1 + \delta\left(\frac{k\epsilon_0 V^2 r}{d^{*2} R^2}\right)^2\right)} < \frac{k\epsilon_0 V^2}{2d^{*2} R^2}; \tag{50}$$

moreover, from (43), (44) and (46), we can easily verify $u_1'(0) \geq u_2'(0)$ and $u_1(R) = u_2(R) = 0$.

Lastly, as Lemma 1 requires, we need to prove that F given by (31) satisfies the Lipschitz condition (37). Thus, starting from (31), $\forall(u(r), v(r)) \in \mathcal{U}$:

$$\begin{aligned}
 & F(r, u(r), u'(r)) - F(r, v(r), v'(r)) \tag{51} \\
 &= \frac{1}{r}u'(r) + \frac{4(1-u(r)-d^*)^2}{\theta\lambda^2(1+\delta|u'(r)|^2)} - \frac{1}{r}v'(r) - \frac{4(1-v(r)-d^*)^2}{\theta\lambda^2(1+\delta|v'(r)|^2)} \\
 &= \frac{1}{r}(u'(r) - v'(r)) + \frac{1}{\theta\lambda^2} \left(\frac{4(1-u(r)-d^*)^2}{1+\delta|u'(r)|^2} - \frac{4(1-v(r)-d^*)^2}{1+\delta|v'(r)|^2} \right) \\
 &= \frac{1}{r}(u'(r) - v'(r)) + \frac{4}{\theta\lambda^2} \left(\frac{(1-u(r)-d^*)^2(1+\delta|u'(r)|^2) - \delta|u'(r)|^2}{1+\delta|u'(r)|^2} \right. \\
 &\quad \left. - \frac{(1-v(r)-d^*)^2(1+\delta|v'(r)|^2) - \delta|v'(r)|^2}{1+\delta|v'(r)|^2} \right) \\
 &= \frac{1}{r}(u'(r) - v'(r)) + \frac{4}{\theta\lambda^2} \left((1-u(r)-d^*)^2 \left(1 - \frac{\delta|u'(r)|^2}{1+\delta|u'(r)|^2} \right) \right. \\
 &\quad \left. - (1-v(r)-d^*)^2 \left(1 - \frac{\delta|v'(r)|^2}{1+\delta|v'(r)|^2} \right) \right) \\
 &= \frac{1}{r}(u'(r) - v'(r)) + \frac{4}{\theta\lambda^2} \left((1-u(r)-d^*)^2 - (1-v(r)-d^*)^2 \right. \\
 &\quad \left. - \frac{(1-u(r)-d^*)^2\delta|u'(r)|^2}{1+\delta|u'(r)|^2} + \frac{(1-v(r)-d^*)^2\delta|v'(r)|^2}{1+\delta|v'(r)|^2} \right).
 \end{aligned}$$

Observing that $\frac{(1-u(r)-d^*)^2\delta|u'(r)|^2}{1+\delta|u'(r)|^2} > 0$, Equation (51) becomes:

$$\begin{aligned}
 & F(r, u(r), u'(r)) - F(r, v(r), v'(r)) \tag{52} \\
 &< \frac{1}{r}(u'(r) - v'(r)) + \frac{4}{\theta\lambda^2} \left((1-u(r)-d^*)^2 \right. \\
 &\quad \left. - (1-v(r)-d^*)^2 + \frac{(1-v(r)-d^*)^2\delta|v'(r)|^2}{1+\delta|v'(r)|^2} \right).
 \end{aligned}$$

Moreover, since $\frac{\delta|v'(r)|^2}{1+\delta|v'(r)|^2} \leq 1$, Equation (52) can be written as

$$\begin{aligned}
 & F(r, u(r), u'(r)) - F(r, v(r), v'(r)) \tag{53} \\
 &< \frac{1}{r}(u'(r) - v'(r)) + \frac{4}{\theta\lambda^2} ((1-u(r)-d^*)^2 \\
 &\quad - (1-v(r)-d^*)^2 + (1-v(r)-d^*)^2).
 \end{aligned}$$

Furthermore, with $(1 - v(r) - d^*)^2 > 0$ from (53)

$$\begin{aligned}
 & F(r, u(r), u'(r)) - F(r, v(r), v'(r)) & (54) \\
 < \frac{1}{r}(u'(r) - v'(r)) + \frac{4}{\theta\lambda^2}((1 - u(r) - d^*)^2 + (1 - v(r) - d^*)^2) \\
 & < \frac{1}{r}(u'(r) - v'(r)) + \frac{4}{\theta\lambda^2}((1 - u(r))^2 + (1 - v(r))^2) \\
 < \frac{1}{r}(u'(r) - v'(r)) + \frac{4}{\theta\lambda^2}(2 + u^2(r) + v^2(r) - 2u(r) - 2v(r)) \\
 & < \frac{1}{r}(u'(r) - v'(r)) + \frac{4}{\theta\lambda^2}(2 + u(r) + v(r) - 2u(r) - 2v(r)) \\
 & = \frac{1}{r}(u'(r) - v'(r)) + \frac{4}{\theta\lambda^2}(2 - u(r) - v(r)) \\
 & < \frac{1}{r}(u'(r) - v'(r)) + \frac{4}{\theta\lambda^2}(2 + u(r) - v(r)).
 \end{aligned}$$

As it is safe to assume that $u(r) > v(r)$, and with $u(r) < 1$ and $v(r) < 1$,

$$2 < \bar{K}(u(r) - v(r)) \tag{55}$$

with $\bar{K} = \bar{K}(r) = \sup\{2/(u(r) - v(r)) \mid (r(r), v(r)) \in \mathcal{U}\}$, from which $\bar{K} \geq \frac{2}{u(r)-v(r)}$ so that (54) becomes

$$\begin{aligned}
 & F(r, u(r), u'(r)) - F(r, v(r), v'(r)) & (56) \\
 < \underbrace{\frac{1}{r}}_{L_1(r)}(u'(r) - v'(r)) + \underbrace{\frac{4(\bar{K}(r) + 1)}{\theta\lambda^2}}_{K_2(r)}(u(r) - v(r)).
 \end{aligned}$$

Moreover,

$$\begin{aligned}
 & F(r, u(r), u'(r)) - F(r, v(r), v'(r)) \tag{57} \\
 &= \frac{1}{r}(u'(r) - v'(r)) + \frac{4(1 - u(r) - d^*)^2}{\theta\lambda^2(1 + \delta|u'(r)|^2)} - \frac{4(1 - v(r) - d^*)^2}{\theta\lambda^2(1 + \delta|v'(r)|^2)} \\
 &= \frac{1}{r}(u'(r) - v'(r)) + \frac{4}{\theta\lambda^2} \left(\frac{(1 - u(r) - d^*)^2}{1 + \delta|u'(r)|^2} - \frac{(1 - v(r) - d^*)^2}{1 + \delta|v'(r)|^2} \right) \\
 &\geq \frac{1}{r}(u'(r) - v'(r)) + \frac{4}{\theta\lambda^2} \left(\frac{(1 - u(r) - d^*)^2}{1 + \delta|u'(r)|^2} - (1 - v(r) - d^*)^2 \right) \\
 &\geq \frac{1}{r}(u'(r) - v'(r)) + \frac{4}{\theta\lambda^2} \left(\frac{(1 - u(r) - d^*)^2}{1 + \delta|u'(r)|^2} - (1 - v(r) - d^*) \right) \\
 &= \frac{1}{r}(u'(r) - v'(r)) + \frac{4}{\theta\lambda^2} \left(\frac{(1 - u(r) - d^*)^2}{1 + \delta|u'(r)|^2} (1 + \delta|u'(r)|^2 \right. \\
 &\quad \left. - \delta|u'(r)|^2) - (1 - v(r) - d^*) \right) \\
 &= \frac{1}{r}(u'(r) - v'(r)) + \frac{4}{\theta\lambda^2} \left((1 - u(r) - d^*)^2 \right. \\
 &\quad \left. - \frac{(1 - u(r) - d^*)^2 \delta|u'(r)|^2}{1 + \delta|u'(r)|^2} - (1 - v(r) - d^*) \right) \\
 &> \frac{1}{r}(u'(r) - v'(r)) + \frac{4}{\theta\lambda^2} \left((1 - u(r) - d^*)^2 \right. \\
 &\quad \left. - (1 - u(r) - d^*)^2 - (1 - v(r) - d^*) \right) \\
 &= \frac{1}{r}(u'(r) - v'(r)) + \frac{4}{\theta\lambda^2} (- (1 - v(r) - d^*)) \\
 &> \frac{1}{r}(u'(r) - v'(r)) + \frac{4}{\theta\lambda^2} (- (1 - v(r) - d^*) - (1 - u(r) - d^*)) \\
 &= \frac{1}{r}(u'(r) - v'(r)) + \frac{4}{\theta\lambda^2} (-1 + v(r) + d^* - 1 + u(r) + d^*) \\
 &= \frac{1}{r}(u'(r) - v'(r)) + \frac{4}{\theta\lambda^2} (-2 + 2d^* + u(r) + v(r)) \\
 &\geq \frac{1}{r}(u'(r) - v'(r)) + \frac{4}{\theta\lambda^2} (-2 + 2d^* + u(r) - v(r)) \\
 &> \frac{1}{r}(u'(r) - v'(r)) + \frac{4}{\theta\lambda^2} (-2 + u(r) - v(r)) \\
 &= \frac{1}{r}(u'(r) - v'(r)) - \frac{8}{\theta\lambda^2} + \frac{4(u(r) - v(r))}{\theta\lambda^2}.
 \end{aligned}$$

Supposing again that $u(r) > v(r)$, Equation (55) holds, from which

$$-8 > -4\bar{K}(r)(u(r) - v(r)); \tag{58}$$

therefore, Equation (57) becomes

$$\begin{aligned}
 F(r, u(r) - v(r), u'(r) - v'(r)) &> \frac{1}{r}(u'(r) - v'(r)) - \frac{8}{\theta\lambda^2} + \frac{4(u(r) - v(r))}{\theta\lambda^2} \tag{59} \\
 &= \frac{1}{r}(u'(r) - v'(r)) + \frac{1}{\theta\lambda^2}(-8 + 4(u(r) - v(r))) \\
 &> \frac{1}{r}(u'(r) - v'(r)) + \frac{1}{\theta\lambda^2}(-4\bar{K}(r)(u(r) - v(r)) + 4(u(r) - v(r))) \\
 &= \underbrace{\frac{1}{r}(u'(r) - v'(r))}_{L_2(r)} + \underbrace{\frac{4 - 4\bar{K}(r)}{\theta\lambda^2}(u(r) - v(r))}_{K_1(r)}.
 \end{aligned}$$

Lastly, it is required that $u'_1(a) \geq u'_2(a)$. For this goal, since $a = r = 0$, we achieve $u'_1(a) = u'_1(0)$. Moreover, $u'_2(a) = u'_2(0) = 0$. Furthermore, $u_1(R) = u_2(R) = 0$. Thus, the proof of the theorem is complete. \square

Remark 6. Physically, as T increases, and V is fixed (if the intended use of the device was chosen), the membrane lifts from its rest position to a lesser extent than that when T is reduced. On the other hand, by increasing p_{el} , the deformation of the membrane is more accentuated. This is confirmed in (42). In fact, from (16),

$$R^2 = 4k_1T \tag{60}$$

and from (17), we obtain

$$\frac{k_1}{k} = \frac{1}{k_2}. \tag{61}$$

Thus, Equation (42) is writable as

$$\theta\lambda^2 > \frac{8Td^{*2}}{k_2\epsilon_0V^2\left(1 + \delta\left(\frac{k_2\epsilon_0V^2r}{4Td^{*2}}\right)^2\right)}. \tag{62}$$

Analyzing (62), increasing T also increases $\theta\lambda^2$, so that, observing (2), $|u''(r)|$ significantly decreases with the consequent reduction in the concavity of the membrane. Furthermore, increasing p_{el} and considering (17) increases k_2 , so that $\theta\lambda^2$ decreases. Then, $|u''(r)|$ in (2) increases. We lastly observe that (42), when $\delta = 0$ (i.e., without fringing field), we obtain the well-known algebraic condition studied in [12].

7. Solution Uniqueness

As verified above, Equation (2) admits at least one solution, $u(r)$, such that $u_1(r) < u(r) < u_2(r)$, where both $u_1(r)$ and $u_2(r)$ satisfy the hypotheses of Theorem 1. However, the uniqueness of the solution is not ensured, as proved in the following theorem.

Theorem 2. If the hypotheses of Theorem 1 regarding (2) are satisfied, and $u_1(r)$ and $u_2(r)$ together satisfy the assigned boundary conditions, then the uniqueness of solution $u(r)$, such that $u_1(r) \leq u(r) \leq u_2(r)$, is not guaranteed.

Proof of Theorem 2. As specified in (54),

$$L_1(r)u'(r) + K_2(r)u(r) = \frac{1}{r}u'(r) + \frac{4(\bar{K}(r) + 1)}{\theta\lambda^2}u(r). \tag{63}$$

Therefore, considering Lemma 2, we can take into account the following ODE:

$$u''(r) + L_1(r)u'(r) + K_2(r)u(r) = 0, \tag{64}$$

which, in our case, since $L_1(r) = \frac{1}{r}$ and $K_2(r) = \frac{4(\overline{K}(r)+1)}{\theta\lambda^2}$, becomes

$$u''(r) + \frac{1}{r}u'(r) + \frac{4(\overline{K}(r)+1)}{\theta\lambda^2}u(r) = 0, \tag{65}$$

which represents a special case of the following Bessel equation:

$$u''(r) + \frac{1}{r}u'(r) + \alpha^2u(r) = 0, \tag{66}$$

with $\alpha = \sqrt{\frac{4(\overline{K}(r)+1)}{\theta\lambda^2}} \in \mathbb{R}^+$. From the Bessel theory of ordinary differential equations, the general solution for (65) can be written in terms of the linear combination of two linearly independent Bessel functions of the first and second kind of the zero-th order, $J_0\left(\sqrt{\frac{4(\overline{K}(r)+1)}{\theta\lambda^2}}r\right)$ and $Y_0\left(\sqrt{\frac{4(\overline{K}(r)+1)}{\theta\lambda^2}}r\right)$, respectively. In other words:

$$u(r) = c_1J_0\left(\sqrt{\frac{4(\overline{K}(r)+1)}{\theta\lambda^2}}r\right) + c_2Y_0\left(\sqrt{\frac{4(\overline{K}(r)+1)}{\theta\lambda^2}}r\right) \tag{67}$$

where c_1 and c_2 are arbitrary constants, and

$$J_0\left(\sqrt{\frac{4(\overline{K}(r)+1)}{\theta\lambda^2}}r\right) = 1 + \sum_{m=1}^{+\infty} \frac{(-1)^m \left(\sqrt{\frac{4(\overline{K}(r)+1)}{\theta\lambda^2}}\right)^{2m}}{2^{2m}(m!)^2} \tag{68}$$

$$\begin{aligned} & Y_0\left(\sqrt{\frac{4(\overline{K}(r)+1)}{\theta\lambda^2}}r\right) \tag{69} \\ &= \frac{2}{\pi} \left[\left(\gamma + \ln\left(0.5\sqrt{\frac{4(\overline{K}(r)+1)}{\theta\lambda^2}}r\right) \right) J_0\left(\sqrt{\frac{4(\overline{K}(r)+1)}{\theta\lambda^2}}r\right) \right. \\ & \quad \left. + \sum_{m=1}^{+\infty} \frac{(-1)^{m+1} H_m \left(\sqrt{\frac{4(\overline{K}(r)+1)}{\theta\lambda^2}}\right)^{2m}}{2^{2m}(m!)^2} \right] \end{aligned}$$

in which $\gamma = 0.5772$ is the Euler–Mascheroni constant, and $H_m = 1 + \frac{1}{2} + \frac{1}{3} + \dots + \frac{1}{m}$. We observe that, for $r \rightarrow 0$, we obtain that $J_0 \rightarrow 1$. Y_0 also has logarithmic singularity when $r = 0$. Therefore, considering a linear combination with $c_2 = 0$ and $c_1 \neq 0$, we obtain the following general solution:

$$u(r) = c_1 \left(1 + \sum_{m=1}^{+\infty} \frac{(-1)^m \left(\sqrt{\frac{4(\overline{K}(r)+1)}{\theta\lambda^2}}\right)^{2m}}{2^{2m}(m!)^2} \right) \tag{70}$$

Equation (70) represents a nontrivial solution for (65). Thus, by Lemma 2, it follows that the uniqueness of the solution to Problem (2) is not guaranteed because a subinterval of $[0, R]$ exists (in our case, itself) on which (64) admits no trivial solution. \square

8. On Research of Critical Points and Stability

8.1. A More Suitable Writing of the Differential Model

For searching any critical points, we need to rewrite (2) as a system of two ordinary differential equations of the first order in normal form [37]. For this purpose, let us consider two functions, $u_1(r)$ and $u_2(r)$, such that

$$u_1(r) = u(r), \quad u_2(r) = u'(r). \tag{71}$$

Then, Equation (71) allows for rewriting (2) as a system of differential equations of the first order in which the unknown functions are the profile of the membrane $u(r)$ and its speed of variation $u'(r)$. In fact, from (2) and considering (71), we can write

$$\begin{cases} u_1'(r) = u_2(r); \\ u_2'(r) = -\frac{1}{r}u_2(r) - \frac{(1-u_1(r)-d^*)^2}{\theta\lambda^2(1+\delta|u_2(r)|^2)} \\ u_1(R) = u_2(0) = 0. \end{cases} \tag{72}$$

8.2. Critical Points and Stability

System (72) is a special case of the following general formulation:

$$\begin{cases} u_1'(r) = \bar{f}(u_1(r), u_2(r)); \\ u_2'(r) = \bar{g}(u_1(r), u_2(r)), \end{cases} \tag{73}$$

where, in our case,

$$\bar{f}(u_1(r), u_2(r)) = u_2(r) \tag{74}$$

and

$$\bar{g}(u_1(r), u_2(r)) = -\frac{1}{r}u_2(r) - \frac{(1-u_1(r)-d^*)^2}{\theta\lambda^2(1+\delta|u_2(r)|^2)}. \tag{75}$$

Therefore, for achieving the critical points, we set $u_1'(r) = u_2'(r) = 0$, which in our case, since $\theta\lambda^2 \neq 0$, we are given the following unique critical point:

$$(u_1^0, u_2^0) = (1 - d^*, 0). \tag{76}$$

To evaluate the stability of (76), we exploit the first Lyapunov criterion [37] that is based on the linearization of System (72) in the neighborhood of the critical point. For this purpose, we consider the following change of variable:

$$u_1(r) = u_1^0 + \epsilon\zeta(r); \quad u_2(r) = u_2^0 + \epsilon\eta(r) \tag{77}$$

with ϵ being a small-enough quantity. Therefore, considering (73)–(75) and (77),

$$\begin{cases} u_1'(r) = \epsilon\zeta'(r) = \bar{f}(u_1(r), u_2(r)) \\ u_2'(r) = \epsilon\eta'(r) = \bar{g}(u_1(r), u_2(r)) \end{cases} \tag{78}$$

from which, developing in Taylor series both $\bar{f}(u_1(r), u_2(r))$ and $\bar{g}(u_1(r), u_2(r))$, and neglecting the terms of an order higher than the linear one and setting $\tau = \sqrt{\zeta^2 + \eta^2}$, it follows that

$$\begin{cases} \epsilon\zeta'(r) = \bar{f}(u_1^0 + \epsilon\zeta(r), u_2^0 + \epsilon\eta(r)) \approx \\ \approx \bar{f}(u_1^0, u_2^0) + \epsilon\bar{f}_{u_1}(u_1^0, u_2^0)\zeta(r) + \epsilon\bar{f}_{u_2}(u_1^0, u_2^0)\eta(r) + o(\tau) \\ \epsilon\eta'(r) = \bar{g}(u_1^0 + \epsilon\zeta(r), u_2^0 + \epsilon\eta(r)) \approx \\ \approx \bar{g}(u_1^0, u_2^0) + \epsilon\bar{g}_{u_1}(u_1^0, u_2^0)\zeta(r) + \epsilon\bar{g}_{u_2}(u_1^0, u_2^0)\eta(r) + o(\tau). \end{cases}$$

Remark 7. Equation (79) makes sense because both $u_1(r)$ and $u_2(r)$ are analytical functions allowing for the linearization procedure by means of computing \bar{f}_{u_1} , \bar{f}_{u_2} , \bar{g}_{u_1} and \bar{g}_{u_2} .

In (79), $\bar{f}(u_1^0, u_2^0) = \bar{g}(u_1^0, u_2^0) = 0$, so that it becomes

$$\begin{cases} \bar{\zeta}'(r) = \bar{f}_{u_1}(u_1^0, u_2^0)\bar{\zeta}(r) + \bar{f}_{u_2}(u_1^0, u_2^0)\eta(r) \\ \eta'(r) = \bar{g}_{u_1}(u_1^0, u_2^0)\bar{\zeta}(r) + \bar{g}_{u_2}(u_1^0, u_2^0)\eta(r). \end{cases} \tag{79}$$

Moreover,

$$\bar{f}_{u_1}(u_1^0, u_2^0) = 0, \quad \bar{f}_{u_2}(u_1^0, u_2^0) = 1, \quad \bar{g}_{u_2}(u_1^0, u_2^0) = -\frac{1}{r} \tag{80}$$

and

$$\bar{g}_{u_1}(u_1^0, u_2^0) = 2(1 - (1 - d^*) - d^*) = 0, \tag{81}$$

so that System (79) can be written as

$$\begin{cases} \bar{\zeta}'(r) = \eta(r) \\ \eta'(r) = -\frac{\eta(r)}{r} \end{cases} \tag{82}$$

that, when solved, gives us

$$\bar{\zeta} + \ln \eta^{C_1} = C_2 \tag{83}$$

with both C_1 and C_2 being constant. Equation (82), indicated by

$$\mathbf{z} = \begin{pmatrix} \bar{\zeta}(r) \\ \eta(r) \end{pmatrix}, \quad \dot{\mathbf{z}} = \begin{pmatrix} \bar{\zeta}'(r) \\ \eta'(r) \end{pmatrix}, \quad A = \begin{pmatrix} 0 & 1 \\ 0 & -\frac{1}{r} \end{pmatrix}, \tag{84}$$

can easily be written as

$$\dot{\mathbf{z}} = A\mathbf{z}. \tag{85}$$

Let us consider the following definitions [38].

Definition 1. If A is a square matrix with order n , with $r \leq n$ distinct eigenvalues $\lambda_1, \lambda_2, \dots, \lambda_r$, $i \neq j$, the characteristic polynomial of A is

$$P(s) = (s - \lambda_1)^{v_1}(s - \lambda_2)^{v_2} \dots (s - \lambda_r)^{v_r} \tag{86}$$

such that $\sum_{i=1}^r v_i = n$. $v_i \in \mathbb{N}^+$ defines the algebraic multiplicity of generic eigenvalue λ_i . Moreover, the geometric multiplicity of λ_i is defined by number μ_i of the linearly independent eigenvectors corresponding to it.

Definition 2. If λ is an eigenvalue of A with algebraic multiplicity v linked to Jordan form \mathbf{J} , the index of λ , π , is the order of the largest Jordan block associated with λ in \mathbf{J} .

Now, we present the following result evaluating the stability of (85) exploiting a criterion on the basis of A eigenvalues [38].

Theorem 3. Dynamic systems in form (85) admit at least one stable equilibrium position if, and only if, its matrix, A , does not have eigenvalues with a positive real part and if any eigenvalues with a real part zero have a unit index. Furthermore, if $\mathbf{z}_0 = [z_{0,1}, z_{0,2}]^T$, then

$$\dot{\mathbf{z}}(r) = e^{Ar} \mathbf{z}(0) = e^{Ar} \mathbf{z}_0. \tag{87}$$

Thus, the following result holds.

Proposition 1. Equation (82) admits a stable equilibrium position.

Proof. From A , two eigenvalues, λ_1 and λ_2 , are computed:

$$\lambda_1 = 0; \quad \lambda_2 = -\frac{1}{r}, \tag{88}$$

so that, by Theorem 3, it follows that System (82) is stable, and (76) is a stable equilibrium position. \square

Remark 8. The number of the eigenvalues of A , counted with their algebraic multiplicity, is equal to the order of A . Moreover, the geometric multiplicity of each eigenvalue is equal to the algebraic multiplicity. Then, it follows that A is diagonalizable [38].

Therefore, since A is diagonalizable (see Remark 8), e^{Ar} can be written as [38]:

$$e^{Ar} = \sum_{k=1}^n \mathbf{t}_k \cdot \mathbf{s}_k^T e^{\lambda_k r} = \mathbf{t}_1 \cdot \mathbf{s}_1 + \mathbf{t}_2 \cdot \mathbf{s}_2 e^{-1} \tag{89}$$

in which \mathbf{t}_k and \mathbf{s}_k are, respectively, the left and right eigenvectors corresponding to λ_k . Thus,

$$\mathbf{t}_1 = [1 \ 0]^T, \quad \mathbf{t}_2 = [1 \ -r^{-1}]^T, \quad \mathbf{s}_1 = [1 \ r], \quad \mathbf{s}_2 = [0 \ 1], \tag{90}$$

so that (89) becomes

$$e^{Ar} = \begin{pmatrix} \frac{1}{r} & r + \frac{1}{e} \\ 0 & -\frac{1}{er} \end{pmatrix}. \tag{91}$$

Moreover, Equation (91) for $r \neq 0$ is limited in norm, so that (87) becomes

$$\begin{cases} \zeta(r) = \frac{\zeta_0}{r} + (r + e^{-1})\eta_0 \\ \eta(r) = -\frac{\eta_0}{re} \end{cases} \tag{92}$$

from which, eliminating r , we achieve

$$\zeta(r)\eta(r) = -\frac{\zeta_0 e \eta^2(r)}{\eta_0} - \frac{\eta_0^2}{e} + \frac{\eta_0}{e} \eta(r). \tag{93}$$

Indicated by

$$H = \begin{pmatrix} -\frac{\zeta_0 e}{\eta_0} & -\frac{1}{2} & 1 \\ -\frac{1}{2} & 0 & 0 \\ 1 & 0 & -\frac{\eta_0^2}{e} \end{pmatrix} \tag{94}$$

and

$$H_1 = \begin{pmatrix} -\frac{\zeta_0 e}{\eta_0} & -\frac{1}{2} \\ -\frac{1}{2} & 0 \end{pmatrix} \tag{95}$$

one easily achieves that $|H| \neq 0$ and $|H_1| < 0$, so that (93) on $\zeta - \eta$ plane represents a hyperbole. Furthermore, from (92),

$$\eta(r) = -\frac{\zeta(r)}{r(er+1)} + \frac{\zeta_0}{r^2(er+1)}, \tag{96}$$

in which $\forall r \in (0, R]$ represents a straight line of which the slope, as r varies on $(0, R]$, changes from $\frac{1}{r(er+1)}$ to $\frac{1}{R(er+1)}$, intercepting point $(\frac{x_{i0}}{r}, 0)$ on axis $\eta(r) = 0$ and point $(0, \frac{x_{i0}}{r^2(1+er)})$ on axis $\zeta(r) = 0$. Therefore, the straight line, when its slope changes, intercepts an arc of hyperbole representing points $(\zeta(r), \eta(r))$. This arc of hyperbole represents the place of points $\zeta(r) - \eta(r)$, which admit stability for (85).

Concerning the stability of System (72), let us introduce the following lemma [37].

Lemma 3. *If linearized System (85) is stable, the critical point of nonlinear System (72) is stable itself.*

Therefore, we can introduce the following important result.

Proposition 2. *Critical point (76) is an equilibrium position characterized by stability for System (72).*

Proof of Proposition 2. It is an immediate consequence of Lemma 3. □

Remark 9. *Point $(1 - d^*, 0)$ identifies a profile of the membrane when u_0 is very close to the upper disk. This poses a risk, as the membrane could touch the upper disk. Electrostatically, considering that*

$$\frac{1}{(1 - u(r))^2} \approx \frac{1}{d^*}, \tag{97}$$

p_{el} becomes

$$p_{el} = \frac{1}{2} \frac{\epsilon_0 V^2}{(1 - u(r))^2} \approx \frac{\epsilon_0 V^2}{2d^*}. \tag{98}$$

Thus, once V is fixed, p_{el} does not fluctuate, so that any variations of p_{el} are not appreciable. Then, from (17), not even any fluctuations of p are appreciable, so that if the membrane reaches the unstable equilibrium position, the risk of touching the upper disk is minimal.

Remark 10. *The only equilibrium position that we obtained was fixed by quantity $1 - d^*$. It was a constant amount once safety distance d^* was set. The greater d^* is, the lower the deformation of the membrane under stable conditions. Obviously, a lower bound is obtained if $d^* = 1$. This lower-bound condition, however, requires that the membrane does not deform despite the application of an electrical voltage V , even of strong amplitude. We, therefore, deduce that the condition of a stable lower bound, even if it has full meaning from a mathematical point of view, from a physical point of view, it has no relevance because it does not admit membrane deformations even if electrostatic stress is relevant.*

9. On Admissible Values of V

9.1. Minimal Value of V to Win the Mechanical Inertia of the Membrane

Proposition 3. *Let us consider Model (2) and its condition of existence (42). Thus, the minimal value of V to win membrane mechanical inertia $(V_{min})_{inertia}$ satisfies the following inequality:*

$$(V_{min})_{inertia} = \sqrt[4]{\frac{Td^{*6}d^3}{\epsilon_0^2 + 4\delta k^2 p_{el}^2}}. \tag{99}$$

Proof of Proposition 3. From (42),

$$\begin{aligned} \lambda^2 &> \frac{2R^2 d^{*2}}{\theta V^2 \epsilon_0 k \left(1 + \delta \left(\frac{k\epsilon_0 V^2 r}{d^{*2} R^2}\right)^2\right)} \geq \frac{2R^2 d^{*2}}{\theta V^2 \epsilon_0 k \left(1 + \delta \left(\frac{k\epsilon_0 V^2}{d^{*2}}\right)^2\right)} = \\ &= \frac{2R^2 d^{*6}}{\theta V^2 \epsilon_0 k (d^{*4} + \delta (k\epsilon_0 V^2)^2)} \geq \frac{2R^2 d^{*6}}{\theta V^2 \epsilon_0 k (d^{*4} + \delta (kV^2)^2)} \end{aligned} \tag{100}$$

from which, considering that [1]

$$\lambda^2 = \frac{2\epsilon_0 V^2 R^2}{d^3 T}, \tag{101}$$

we achieve

$$\frac{2\epsilon_0 V^2 R^2}{d^3 T} \geq \frac{2R^2 d^{*6}}{\theta V^2 \epsilon_0 k (d^{*4} + \delta (kV^2)^2)}, \tag{102}$$

and again

$$V^4(d^{*4} + \delta(kV^2)^2) \geq \frac{Td^{*6}d^3}{\theta k\epsilon_0^2}. \tag{103}$$

However, from (18),

$$kV^2 = \frac{2kp_{el}(d - u(r))^2}{\epsilon_0} \tag{104}$$

from which

$$1 + \delta(kV^2)^2 = 1 + \frac{4\delta k^2 p_{el}^2 (d - u(r))^4}{\epsilon_0^2}, \tag{105}$$

so that (103) becomes

$$V^4(1 + \delta(kV^2)^2) = V^4\left(1 + \frac{4\delta k^2 p_{el}^2 (d - u(r))^4}{\epsilon_0^2}\right) \geq \frac{Td^{*6}d^3}{\theta k\epsilon_0^2} \tag{106}$$

from which, with $\theta k < 1$ and $d - u(r) < 1$, we can write

$$V^4 \geq \frac{Td^{*6}d^3}{\theta k(\epsilon_0^2 + 4\delta k^2 p_{el}^2 (d - u(r))^4)} \geq \frac{Td^{*2}d^3}{\epsilon_0^2 + 4\delta k^2 p_{el}^2} \tag{107}$$

and

$$V \geq \sqrt[4]{\frac{Td^{*6}d^3}{\epsilon_0^2 + 4\delta k^2 p_{el}^2}} \tag{108}$$

obtaining the (99). \square

Remark 11. Equation (99) makes sense because T appears in the numerator of its right side, i.e., the mechanical tension of the membrane at rest. Then, the greater T is, the greater V must be to overcome the mechanical inertia of the membrane.

9.2. Maximal Value of V so the Membrane Does Not Touch the Upper Disk

Remark 12. Equation (21) was obtained by exploiting the theory of elasticity of circular membranes [1] when external V is applied. Since the considered device is circular, Equation (21) retains its validity and the geometry has axial symmetry (with axis $r = 0$). This symmetry was maintained even in the presence of a fringing field because this phenomenon (more evident at the edges of the device) was also symmetrical with respect to the same vertical axis. Therefore, the presence of the fringing field would seem not to invalidate the validity of (21). However, in (21), there is no trace of C_{el} which represents the most influenced electrostatic parameter by the fringing-field effect, so the presence of terms due in the fringing field is not explicitly evident. On the other hand, studying the existence of the solution for (2), made (21) provide an algebraic condition in which the fringing field (presence of δ) was evident. It follows that, even in the presence of a fringing field, Equation (21) is still valid. Therefore, the achieved results in [12] and concerning the maximal value of V are still valid.

In particular, the following results hold [12].

Proposition 4. Indicating by $(V_{max})_{permissible}$ the maximum value of V in order that the membrane does not touch the upper desk, for Model (2), the following inequality holds (for details, see [12]):

$$(V_{max})_{permissible} < \sqrt{\frac{2d^*(1 - d^*)}{k\epsilon_0}} \tag{109}$$

Thus, considering both (108) and (109), the range of the admissible values for V is

$$\sqrt[4]{\frac{Td^{*6}d^3}{\epsilon_0^2 + 4\delta k^2 p_{el}^2}} \leq V < \sqrt{\frac{2d^*(1-d^*)}{k\epsilon_0}}. \tag{110}$$

Remark 13. Then, Equation (110) makes sense because

$$\sqrt[4]{\frac{Td^{*6}d^3}{\epsilon_0^2 + 4\delta k^2 p_{el}^2}} < \sqrt{\frac{2d^*(1-d^*)}{k\epsilon_0}}. \tag{111}$$

In fact, if absurdly

$$\sqrt[4]{\frac{Td^{*6}d^3}{\epsilon_0^2 + 4\delta k^2 p_{el}^2}} > \sqrt{\frac{2d^*(1-d^*)}{k\epsilon_0}}, \tag{112}$$

one would obtain

$$\delta < \underbrace{\epsilon_0^2 \left(\frac{Td^3 k^2 d^{*4}}{4(1-d^*)^2} - 1 \right)}_{<0} \frac{1}{4k^2 p_{el}^2} \tag{113}$$

so that $\delta < 0$, which represents an impossible condition because $\delta \in \mathbb{R}^+$. Therefore, Equation (111) makes sense, so that (110) is true.

10. Interesting Optimal Control Conditions

If the membrane is at rest, its distance from the upper disk is d , and the C_{el} of the device along any plane whose support is the straight line $r = 0$, in presence of fringing field, is [30]

$$(C_{el})_{curve} = \frac{2\epsilon_0 R}{d} \left\{ 1 + \frac{d}{2\pi R} \ln \left(\frac{2\pi R}{d} \right) \right\}, \tag{114}$$

where d_1 represents the distance so that the total C_{el} , $(C_{el})_{total}$, becomes:

$$(C_{el})_{total} = \int_0^\pi Z(\phi) (C_{el})_{curve} d\phi = (C_{el})_{curve} \int_0^\pi Z(\phi) d\phi. \tag{115}$$

in which $Z(\phi)$ is a bounded and a continuous electrostatic function depending on angular coordinate ϕ [39]. Thus, $Z(\phi)$ being both continuous and bounded,

$$\int_0^\pi Z(\phi) d\phi = D < +\infty, \tag{116}$$

so that (115) becomes

$$(C_{el})_{total} = (C_{el})_{curve} D = \frac{2\epsilon_0 R D}{d} \left\{ 1 + \frac{d}{2\pi R} \ln \left(\frac{2\pi R}{d} \right) \right\}. \tag{117}$$

Thus, the potential energy (indicated by $W_{initial}$) when the device is at rest is

$$W_{initial} = \frac{1}{2} (C_{el})_{total} V^2 = \frac{\epsilon_0 R D V^2}{d} \left\{ 1 + \frac{d}{2\pi R} \ln \left(\frac{2\pi R}{d} \right) \right\}. \tag{118}$$

If the membrane deforms, and in the presence of a fringing field, C_{el}^{def} , along with any curve obtained by intersecting the profile of the deformed membrane with any plane of which the support is line $r = 0$, would become [30]

$$(C_{el}^{def})_{curve} = 2\epsilon_0 R \int_{-R}^{+R} \frac{dr}{d-u(r)} \left\{ 1 + \frac{1}{2\pi R \int_{-R}^{+R} \frac{dr}{d-u(r)}} \ln \left(2\pi R \int_{-R}^{+R} \frac{dr}{d-u(r)} \right) \right\}. \tag{119}$$

However,

$$\frac{1}{d - u(r)} \leq \frac{1}{d^*} \tag{120}$$

from which

$$\int_{-R}^{+R} \frac{dr}{d - u(r)} \leq \int_{-R}^{+R} \frac{dr}{d^*} = \frac{2R}{d^*}. \tag{121}$$

Thus,

$$(C_{el}^{def})_{curve} \leq \frac{4\epsilon_0 R^2}{d^*} \left\{ 1 + \frac{1}{2\pi R \int_{-R}^{+R} \frac{dr}{d - u(r)}} \ln \left(\frac{4\pi R^2}{d^*} \right) \right\}. \tag{122}$$

Moreover,

$$d - u(r) \leq d, \tag{123}$$

from which

$$\frac{1}{d - u(r)} \geq \frac{1}{d} \tag{124}$$

and

$$\int_{-R}^{+R} \frac{dr}{d - u(r)} \geq \int_{-R}^{+R} \frac{dr}{d} \tag{125}$$

Thus, Equation (122), considering (125), becomes

$$(C_{el}^{def})_{curve} \leq \frac{4\epsilon_0 R^2}{d^*} \left\{ 1 + \frac{d}{4\pi R^2} \ln \left(\frac{4\pi R^2}{d^*} \right) \right\}. \tag{126}$$

Therefore, as (117),

$$(C_{el}^{def})_{total} \leq \frac{4\epsilon_0 R^2 D}{d^*} \left\{ 1 + \frac{d}{4\pi R^2} \ln \left(\frac{4\pi R^2}{d^*} \right) \right\}. \tag{127}$$

From (127), considering (109), it follows that

$$W_{final} = \frac{1}{2} (C_{el}^{def})_{total} V^2 \leq \frac{2\epsilon_0 R^2 D}{d^*} \frac{2d^*(1 - d^*)}{k\epsilon_0} \left\{ 1 + \frac{d}{4\pi R^2} \ln \left(\frac{4\pi R^2}{d^*} \right) \right\}. \tag{128}$$

from which

$$(W_{final})_{max} = \frac{2\epsilon_0 R^2 D}{d^*} \frac{2d^*(1 - d^*)}{k\epsilon_0} \left\{ 1 + \frac{d}{4\pi R^2} \ln \left(\frac{4\pi R^2}{d^*} \right) \right\}. \tag{129}$$

Thus, considering both (118) and (129),

$$\begin{aligned} \Delta W &= (W_{final})_{max} - W_{initial} \leq \tag{130} \\ &\leq \frac{2\epsilon_0 R^2 D}{d^*} \frac{2d^*(1 - d^*)}{k\epsilon_0} \left\{ 1 + \frac{d}{4\pi R^2} \ln \left(\frac{4\pi R^2}{d^*} \right) \right\} - \\ &\quad - \frac{\epsilon_0 R D V^2}{d} \left\{ 1 + \frac{d}{2\pi R} \ln \left(\frac{2\pi R}{d} \right) \right\} \end{aligned}$$

On the other hand, from (110),

$$V^2 > \sqrt{\frac{T d^{*6} d^3}{\epsilon_0^2 + 4\delta k^2 p_{el}^2}}; \tag{131}$$

thus,

$$\Delta W > \epsilon_0 RD \sqrt{\frac{Td^*6d^3}{\epsilon_0^2 + 4\delta k^2 p_{el}^2}} \left\{ \frac{2R}{d^*} \left[1 + \frac{d}{4\pi R^2} \ln \left(\frac{4\pi R^2}{d^*} \right) \right] - \frac{1}{d} \left[1 + \frac{d}{2\pi R} \ln \left(\frac{2\pi R}{d} \right) \right] \right\}. \tag{132}$$

10.1. *V Maximizing Δ W*

From (130), it is clear that we obtain an upper limitation for the value of *V*, which maximizes Δ*W* is (*V*_{max})_{permissible}.

10.2. *An Interesting Limitation for ΔW Starting from |E|*

From the equations of Models (22) and (2):

$$\frac{\lambda^2}{(1-u(r))^2} (1 + \delta |u'(r)|^2) = \frac{u'(r)}{r} + \frac{1}{\theta \lambda^2} \frac{(1-u(r)-d^*)^2}{(1 + \delta |u'(r)|^2)}. \tag{133}$$

Considering that $\frac{\lambda^2}{(1-u(r))^2} = \theta |E|^2$, Equation (133) becomes:

$$|E|^2 (1 + \delta |u'(r)|^2) = \frac{u'(r)}{r\theta} + \frac{1}{\theta^2 \lambda^2} \frac{(1-u(r)-d^*)^2}{(1 + \delta |u'(r)|^2)}, \tag{134}$$

so that

$$W_{final} = \frac{1}{2} \epsilon_0 |E|^2 = \frac{\epsilon_0}{2} \left(\frac{u'(r)}{r\theta(1 + \delta |u'(r)|^2)} + \frac{1}{\theta^2 \lambda^2} \frac{(1-u(r)-d^*)^2}{(1 + \delta |u'(r)|^2)^2} \right). \tag{135}$$

Therefore, considering both (118) and (135),

$$\begin{aligned} \Delta W &= W_{final} - W_{initial} = \\ &= \frac{\epsilon_0}{2} \left(\frac{u'(r)}{r\theta(1 + \delta |u'(r)|^2)} + \frac{1}{\theta^2 \lambda^2} \frac{(1-u(r)-d^*)^2}{(1 + \delta |u'(r)|^2)^2} \right) - \\ &\quad - \frac{\epsilon_0 RD V^2}{d} \left\{ 1 + \frac{d}{2\pi R} \ln \left(\frac{2\pi R}{d} \right) \right\}. \end{aligned} \tag{136}$$

Moreover, with $1-u(r)-d^* < 1-d^*$ and $u'(r) < H \in \mathbb{R}^+$ (see, [11,12]), Equation (136) becomes:

$$\begin{aligned} \Delta W &= W_{final} - W_{initial} < \\ &< \frac{\epsilon_0}{2} \left(\frac{H}{r\theta(1 + \delta |u'(r)|^2)} + \frac{1}{\theta^2 \lambda^2} \frac{(1-d^*)^2}{(1 + \delta |u'(r)|^2)^2} \right) - \\ &\quad - \frac{\epsilon_0 RD V^2}{d} \left\{ 1 + \frac{d}{2\pi R} \ln \left(\frac{2\pi R}{d} \right) \right\}. \end{aligned} \tag{137}$$

Lastly, with

$$\frac{1}{1 + \delta |u'(r)|^2} \leq 1 \tag{138}$$

Equation (137) becomes

$$\Delta W < \frac{\epsilon_0}{2} \left(\frac{H}{r\theta} + \frac{(1-d^*)^2}{\theta^2 \lambda^2} \right) - \frac{\epsilon_0 RD V^2}{d} \left\{ 1 + \frac{d}{2\pi R} \ln \left(\frac{2\pi R}{d} \right) \right\}. \tag{139}$$

In (139), the right side is non-negative. In fact, if it were negative, we would easily achieve

$$H < r\theta \left\{ \frac{2RDV^2}{d} \left[1 + \frac{d}{2\pi R} \ln \left(\frac{2\pi R}{d} \right) \right] - \frac{(1-d^*)^2}{\theta^2 \lambda^2} \right\} \quad (140)$$

from which, substituting the usual values for each parameter, we would find that H was increased by a very small non-negative quantity. This means that the slope of the membrane at the edges is very small, as if the deformation of the membrane was extremely small even for high values of V . It is evident that this condition is physically impossible. Hence, it follows that the right side of (139) is always a non-negative quantity.

11. Conclusions

In this study, a new nonlinear second-order differential 2D model for a membrane MEMS device in which fringing-field effects occur was presented and discussed. Once the possibility of formulating $|\mathbf{E}|$ in terms of average membrane curvature was justified, the mathematical model was detailed from the point of view of the actuator, highlighting the link between p and p_{el} , highlighting the actuator–transducer duality. Once two important lemmas were presented, the existence of at least one solution for the proposed model was ensured if an algebraic condition depending on fringing-field parameter δ was verified. However, even if the uniqueness of the solution was not assured, the only permitted equilibrium position of the model is stable. Furthermore, this equilibrium position is associated with the profile of the membrane that was closest to the upper disk; therefore, even if the membrane was very close to the upper disk, the stability of this equilibrium configuration reduced the risk of touching the upper disk. The range of possible values for V was obtained by taking into account the need, on the one hand, to overcome the mechanical inertia of the membrane and, on the other, to prevent the membrane from touching the upper disk, highlighting that the fringing-field effect appeared explicitly only in the extreme of V , delegated to overcome the mechanical inertia of the membrane. Lastly, some conditions for optimal membrane control were obtained. In particular, an increase was obtained for ΔW when the membrane passed from the rest position to a generic deformed configuration. This is very interesting because it contains all the parameters that came into play when the fringing-field phenomenon occurs. Sophisticated mathematical models describing the behavior of the membrane under the effect of V and in the presence of fringing fields, while offering excellent food for thought, are poorly suited to real-time industrial applications. Then, some simplifications of the model and, in our case, of the formulation of the mean curvature, appear necessary. Locally, this is proportional to $|\mathbf{E}|$, but determines the effective deformation of the membrane inside the device. However, the study of the model, although it does not provide results that can be superimposed with experimental data, certainly provides qualitative indications on the electromechanical behavior of a membrane MEMS device. Lastly, the mathematical models adhering to the physical reality of MEMS modeling are extremely complex and obviously do not allow for in-depth analytical studies. Then, some simplifications in the geometry of the devices are necessary to obtain simplified analytical models so that they can be easily studied. Obviously, the results obtained by studying the model proposed in this paper poorly agree with any experiment results, but provide interesting qualitative indications of the behavior of MEMS device membranes characterized by simplified geometries.

Author Contributions: Conceptualization, M.V. and L.F.; methodology, M.V. and L.F.; validation, L.F. and P.D.B.; formal analysis, M.V. and L.F.; investigation, M.V.; resources, L.F.; writing—original draft preparation, M.V.; writing—review and editing, L.F. and P.D.B.; supervision, L.F. and P.D.B. Luisa Fattorusso is Member of the National Group for Mathematical Analysis, Probability, and their Applications (GNAMPA-INdAM). All authors have read and agreed to the published version of the manuscript.

Funding: This research received no external funding.

Conflicts of Interest: The authors declare no conflict of interest.

Abbreviations

The following abbreviations are used in this manuscript:

r	radial coordinate
R	radius of the membrane
$u(r)$	profile of the membrane
V	external voltage
λ^2	parameter depending on V
d	distance between the parallel disks
\mathbf{E}	electrostatic field
θ	coefficient of proportionality between $u''(r)$ and $ \mathbf{E} ^2$
δ	parameter concerning the fringing field effect
$K(r, u(r))$	mean curvature of the membrane
d^*	critical security distance
$(V_{min})_{inertia}$	V to win the mechanical inertia of the membrane
$(V_{max})_{permissible}$	V to avoid that the membrane touches the upper disk
p_{el}	electrostatic pressure
ϵ_0	permittivity of the free space
C_{el}	electrostatic capacitance
p	mechanical pressure
ρ	density
h	thickness of the plate
T	mechanical tension of the membrane at rest
Y	Young modulus
ν	Poisson ratio
u_0	displacement at the center of the membrane
f_{el}	electrostatic force
k_1	coefficient of proportionality between u_0 and p
k_2	coefficient of proportionality between p_{el} and p
k	coefficient of proportionality between u_0 and p_{el}
$u_1(r), u_2(r)$	twice continuously differentiable functions (upper and lower solutions)
$K_1(r), K_2(r), L_1(r), L_2(r)$	continuous functions
$Z(\phi)$	bounded and continuous electrostatic function
$(C_{el})_{curve}$	total electrostatic capacitance when the membrane is at rest
D	constant
$(C_{el}^{def})_{curve}$	electrostatic capacitance when the membrane is deformed
$(C_{el}^{def})_{total}$	total electrostatic capacitance when the membrane is deformed

References

1. Pelesko, J.A.; Bernstein, D.H. *Modeling MEMS and NEMS*; Chapman and Hall, CRC Press Company: Boca Raton, FL, USA; London, UK; New York, NY, USA; Washington, DC, USA, 2003.
2. Gad-el-Hak, M. *MEMS: Design and Fabrication*; Chapman and Hall, CRC Taylor and Francis: Boca Raton, FL, USA, 2006.
3. Cauchi, M.; Grech, I.; Mallia, B.; Mollicone, P.; Sammut, N. Analytical, Numerical and Experimental Study of a Horizontal Electrothermal MEMS Microgripper for the Deformability Characterization of Human Red Blood Cells. *Micromachines* **2018**, *9*, 108. [[CrossRef](#)] [[PubMed](#)]
4. Nathanson, H.; Newell, W.; Wickstrom, R.; Lewis, J. The Resonant Gate Transistor. *IEEE Trans. Electron Devices* **1964**, *14*, 117–133. [[CrossRef](#)]
5. Cassani, D.; Tarsia, A. Periodic Solutions to Nonlocal MEMS Equations. *Discret. Contin. Dyn. Syst. Ser. S* **2016**, *12*, 188–199. [[CrossRef](#)]
6. Cassani, D.; do Ó, J.M.; Ghossoub, N. On a Fourth Order Elliptic Problem with a Singular Nonlinearity. *Nonlinear Stud.* **2009**, *9*, 189–209. [[CrossRef](#)]
7. Zhang, Y.; Wang, T.; Luo, A.; Hu, Y.; Li, X.; Wang, F. Micro Electrostatic Energy Harvester with both Broad Bandwidth and High Normalized Power Density. *Appl. Energy* **2018**, *212*, 363–371. [[CrossRef](#)]
8. Mohammadi, A.; Ali, N. Effect of High Electrostatic Actuation on Thermoelastic Damping in Thin Rectangular Microplate Resonators. *J. Theor. Appl. Mech.* **2015**, *53*, 317–329. [[CrossRef](#)]

9. Vinyas, M.; Kattimani, S. Investigation of the Effect of $BaTiO_3 - CoFe_{24}$ Particle Arrangement on the Static Response of Magneto-Electro-Thermo-Elastic Plates. *Compos. Struct.* **2018**, *185*, 51–56. [[CrossRef](#)]
10. Feng, J.; Liu, C.; Zhang, W.; Hao, S. Static and Dynamic Mechanical Behaviors of Electrostatic MEMS Resonator with Surface Processing Error. *Micromachines* **2018**, *9*, 34.
11. Di Barba, P.; Fattorusso, L.; Versaci, M. Electrostatic Field in Terms of Geometric Curvature in Membrane MEMS Devices. *Commun. Appl. Ind. Math.* **2017**, *8*, 165–184.
12. Di Barba, P.; Fattorusso, L.; Versaci, M. A 2D Non-Linear Second-Order Differential Model for Electrostatic Circular Membrane MEMS Devices: A Result of Existence and Uniqueness. *Mathematics* **2019**, *7*, 1193.
13. Pelesko, J.A.; Driscoll, T.A. The Effect of the Small-Aspect-Ratio Approximation on Canonical Electrostatic MEMS Models. *J. Eng. Math.* **2005**, *53*, 129–152. [[CrossRef](#)]
14. Angiulli, G.; Jannelli, A.; Morabito, F.C.; Versaci, M. Reconstructing the Membrane Detection of a 1D Electrostatic-Driven MEMS Device by the Shooting Method: Convergence Analysis and Ghost Solutions Identification. *Comp. Appl. Math.* **2018**, *37*, 4484–4498. [[CrossRef](#)]
15. Versaci, M.; Angiulli, G.; Fattorusso, L.; Jannelli, A. On the Uniqueness of the Solution for a Semi-Linear Elliptic Boundary Value Problem of the Membrane MEMS Device for Reconstructing the Membrane Profile in Absence of Ghost Solutions. *Int. J. Non-Linear Mech.* **2019**, *109*, 24–31. [[CrossRef](#)]
16. Versaci, M.; Jannelli, A.; Angiulli, G. Electrostatic Micro-Electro-Mechanical-Systems (MEMS) Devices: A Comparison Among Numerical Techniques for Recovering the Membrane Profile. *IEEE Access* **2020**, *8*, 125874–125886. [[CrossRef](#)]
17. Versaci, M.; Di Barba, P.; Morabito, F.C. Curvature-Dependent Electrostatic Field as a Principle for Modelling Membrane-Based MEMS Devices. A Review. *Membranes* **2020**, *10*, 361.
18. Versaci, M.; Morabito, F.C. Membrane Micro Electro-Mechanical Systems for Industrial Applications. In *Handbook of Research on Advanced Mechatronic Systems and Intelligent Robotics*; IGI Global: Hershey, PA, USA, 2003; pp. 139–175.
19. Zozulya, V.V.; Saez, A. A High-Order Theory of a Thermoelastic Beams and Its Application to the MEMS/NEMS Analysis and Simulations. A Review. *Arch. Appl. Mech.* **2016**, *86*, 1255–1273. [[CrossRef](#)]
20. Zega, V.; Frangi, A.; Guercilena, A.; Gattere, G. Analysis of Frequency Stability and Thermoelastic Effects for Slotted Tuning Fork MEMS Resonators. *Sensors* **2018**, *8*, 2157.
21. Sravani, K.G.; Narayana, T.L.; Guha, K.; Rao, K.S. Role of Dielectric Layer and Beam Membrane in Improving the Performance of Capacitive RF MEMS Switches for Ka-Band Applications. *Math. Technol.* **2018**, *9*, 145–156. [[CrossRef](#)]
22. Neff, B.; Casset, F.; Millet, A.; Agache, V.; Verplanck, N.; Boizot, F.; Fanget, S. Development and Characterization of MEMS Membrane Based on Thin-Film PZT Actuators for Microfluidic Applications. In Proceedings of the 19th International Conference on Thermal, Mechanical and Multi-Physics Simulation and Experiments in Microelectronics and Microsystems (EuroSimE), Toulouse, France, 15–18 April 2018.
23. Javaher, H.; Ghanati, P.P.; Azizi, S. A Case Study on the Numerical Solution and Reduced Order Model of MEMS. *Sensors* **2018**, *19*, 35–48. [[CrossRef](#)]
24. de Oliveira Hansen, R.; Mátéfi-Tempfli, M.; Safonovs, R.; Adam, J.; Chemnitz, S.; Reimer, T.; Wagner, B.; Benecke, W.; Mátéfi-Tempfli, S. Magnetic Films for Electromagnetic Actuation in MEMS Switches. *Microsyst. Technol.* **2018**, *24*, 1987–1994. [[CrossRef](#)]
25. Di Barba, P.; Wiak, S. *MEMS: Field Models and Optimal Design*; Springer International Publishing: Berlin/Heidelberg, Germany, 2020.
26. Di Barba, P.; Gotszalk, T.; Majastrzyk, W.; Mognasti, M.; Orłowska, K. Optimal Design of Electromagnetically Actuated MEMS Cantilevers. *Sensors* **2018**, *18*, 2533. [[CrossRef](#)] [[PubMed](#)]
27. Velosa-Moncada, L.A.; Aguilera-Cortés, L.A.; González-Palacios, M.A.; Raskin, J.P.; Herrera-May, A.L. Design of a Novel MEMS Microgripper with Rotatory Electrostatic Comdrive Actuators for Biomedical Applications. *Sensors* **2018**, *18*, 1664.
28. Nisar, A.; Afzulpurkar, N.; Mahaisavariya, B.; Tuantranont, A. MEMS-Based Micropumps in Drug Delivery and Biomedical Applications. *Sens. Actuators B Chem.* **2008**, *2*, 917–942. [[CrossRef](#)]
29. Wei, J.; Ye, D. On MEMS Equation with Fringing Field. *Proc. Am. Math. Soc.* **2010**, *138*, 1693–1699. [[CrossRef](#)]
30. Leus, V.; Elata, D. Fringing Field Effect in Electrostatic Actuator. In *Technical Report ETR-2004-2*; Israel Institute of Technology, Faculty of Mechanical Engineering: Haifa, Israel, 2004.
31. Hosseini, M.; Zhu, G.; Peter, Y.A. A New Formulation of Fringing Capacitance and its Application to the Control of Parallel-Plate Electrostatic Micro Actuators. *Analog. Integr. Circ. Sig. Process.* **2007**, *53*, 119–128. [[CrossRef](#)]
32. Li, Y.; Li, H.; Pickard, F.C., IV; Narayanan, B.; Sen, F.G.; Chan, M.K.; Sankaranarayanan, S.K.; Brooks, B.R.; Roux, B. Machine Learning Force Field Parameters from Ab Initio Data. *J. Chem. Theory Comput.* **2017**, *13*, 4492–4503. [[CrossRef](#)]
33. Imani, M.; Ghoreishi, S.F. Scalable Inverse Reinforcement Learning Through Multi-Fidelity Bayesian Optimization. *IEEE Trans. Neural Netw. Learn. Syst.* **2021**, 1–8. [[CrossRef](#)]
34. Roudneshin, M.; Sayrafian-Pour, K.; Aghdam, A. A Machine Learning Approach to the Estimation of Near-Optimal Electrostatic Force in Micro Energy-Harvesters. In Proceedings of the 2019 IEEE International Conference on Wireless for Space and Extreme Environments, Ottawa, ON, Canada, 16–18 October 2019.
35. Timoshenko, S.; Woinowsky-Krieger, S. *Theory of Plates and Shells*; McGraw Hill: New York, NY, USA, 1959.
36. Bayley, P.B.; Shampine, L.F.; Waltman, P.E. *Nonlinear Two Point Boundary Value Problems*; Academic Press: Cambridge, MA, USA, 1968.
37. Di Barba, P.; Fattorusso, L.; Versaci, M. Curvature Dependent Electrostatic Field in the Deformable MEMS Device: Stability and Optimal Control. *Commun. Appl. Ind. Math.* **2020**, *11*, 35–54.

-
38. Barreira, L.; Valls, C. *Dynamical Systems*; Springer: London, UK, 2020.
 39. Fujimoto, M. *Physics of Classical Electromagnetism*; Springer: New York, NY, USA, 2007.